MULTIPLE-TRANSIENT SURFACE WAVE PHASE VELOCITY ANALYSIS IN EXPANDED f-k DOMAIN AND ITS APPLICATION

HONGYAN SHEN[1,2], CHEN CHEN[2], YUEYING YAN[1] and BAOWEI ZHANG[3]

[1] *School of Earth Sciences and Engineering, Xi'an Shiyou University, Xi'an Shaanxi 710065, P.R. China.*
[2] *Mewbourne College of Earth and Energy, University of Oklahoma, Norman, OK 73019, U.S.A.*
[3] *Langfang Geophysical and Geochemical Exploration Institute, Langfang, Hebei 065000, P.R. China.*

(Received January 8, 2016; revised version accepted June 2, 2016)

ABSTRACT

Shen, H., Chen, C., Yan, Y. and Zhang, B., 2016. Multiple-transient surface wave phase velocity analysis in expanded f-k domain and its application. *Journal of Seismic Exploration*, 25: 299-319.

Surface waves are usually regarded as noise in traditional reflection seismic processing. However, useful and important signals can be extracted from surface waves since it still carries geological information. In this paper, we developed a new method of multiple-transient surface wave phase velocity analysis, which is based on 2D Fourier Transform theory. We established the equation of surface wave velocity analysis in expanded f-k domain to demonstrate the relationship among frequency, wave number, phase velocity, wavelength, and penetration depth. It is more convenient to obtain a relevant velocity spectrum by converting f-k spectrum into the depth-phase velocity (H-v_R) spectrum. We obtained better results by extracting the phase velocity and depth information from the H-v_R spectrum. This has the ability to extract the near-surface geological information with high accuracy and strong capabilities of de-noising. We used the new method to test an actual dataset for detecting active faults. The study shows that Rayleigh wave phase velocity has the ability to delineate structures in the near surface, about 150 m deep, which is very useful to deal with geological structures in Quaternary geology, such as bedrock fractures. The geological structures interpreted from the Rayleigh wave phase velocity profile and reflection seismic cross-section show a strong consistency.

KEY WORDS: surface waves, reflection seismic, 2D Fourier transform, phase velocity analysis, dispersion curve, near-surface structure.

0963-0651/16/$5.00

INTRODUCTION

In reflection seismic exploration, the acquired seismic data often presents surface waves with characteristics of low frequency, low apparent velocity, high amplitude and frequency dispersion, which comes from the free surface (Rayleigh, 1887; Xia et al., 1999, 2014). For a long time, researchers only used reflected wave information in traditional seismic processing techniques. In order to improve the quality in reflection seismic imaging, it is critical to eliminate or suppress the strong interference noise of surface waves during data processing. In recent years, some researchers realized that the surface waves in reflection seismic data also have attractive application prospects (Mari, 1984; Claudio et al., 2010; Stobbia et al., 2011; Shen and Li, 2014). Mari (1984) did inversion experiments of the surface structure for shear wave static correction using the Love-wave dispersion in transverse records. In order to improve the imaging quality of P-S converted waves, Ritzwoller and Levshin (2002) presented a multi-wave inversion (MWI) method that was designed to use a wide variety of information in marine seismic data, which also included surface waves. Strobbia et al. (2010) used surface waves in reflection seismic data to invert the near-surface characteristics from static correction and noise removal processing for the Lower Fars oil field in Kuwait. Stobbia et al. (2011) conducted several case studies to do the comparison and discussion by excluding and re-using surface waves. Considering the surface waves and guided waves were not noises, but a type of useful signal that can be extracted from the reflected seismic records and exploited for a variety of well-established geophysical solutions, Boiero et al. (2013) provided a workflow for the analysis and joint inversion of the surface and guided waves in both land and offshore seismic data. Shen and Li proposed a Rayleigh wave processing method in 2014. All of these studies can be expanded to the real data application of surface waves.

Surface wave propagation relates to near-surface velocity. Surface waves can be used to reveal subsurface structures or geological anomaly targets by imagining the velocity variation. How to extract the accurate and reliable surface wave velocity is one of the keys for surface wave exploration. In order to effectively extract the geological information in surface waves, Stokoe and Nazarian (1983) presented an excellent surface wave processing technique, Spectral Analysis of Surface Wave (SASW), which was used to analyze the dispersion curve of surface waves. Gucunski and Woods (1992) carried out an analytical simulation of SASW. In 1996, Matthews et al. summarized the SASW technique by doing a few examples. The SASW technique is a cross-correlation method to calculate the dispersion curve of surface waves from two-channel receiver seismic data. Although the lateral resolution for this method is relatively high, 360° phase winding occurs during unwrapping phases. In addition, SASW cannot get the dispersion curve of higher modes, which results in a shallower detecting depth (Jia et al., 2010).

Park et al. (1996, 1998, 1999) and Xia et al. (1999, 2005, 2014) developed a high frequency surface wave processing method, Multichannel Analysis of Surface Wave (MASW), to extract surface wave dispersion curves. Furthermore, S-waves velocity can be obtained with dispersion curve inversion. So far, MASW is one of the most commonly used methods to determine S-wave velocity in geotechnical and environmental engineering. The MASW method is a multi-channel high-frequency transient surface wave data processing technique, which converts the seismic records from the time-space (t-x) domain to frequency-wave number (f-k) domain or phase velocity-frequency (v_R-f) domain by 2D Fast Fourier Transform (2D FFT). The method not only takes advantage of high and low frequency information to detect formation targets, but also can get multi-mode surface wave dispersion curves to make it possible to get finer stratum structure (Xia et al., 1999; Jia et al., 2010). Strobbia and Foti (2006) also proposed a method of multi-offset phase analysis (MOPA) with adopting the f-k transform for surface waves.

Currently, the f-k transform is widely used in multiple-transient surface wave data processing. Frequency and propagation velocity of surface waves disperse with other seismic wave properties. Surface waves also have the characteristic of dispersion that frequency changes with velocity (Haskell, 1953). So it is fairly easy to obtain the dispersion curve by searching the peaks of the amplitude spectrum with the surface wave data transforming from the time-space domain into frequency-wave number domain, frequency-slowness domain or frequency-phase velocity (McMechan and Yedlin, 1981; Gabriels et al., 1987; Park et al., 1999). Although these methods are very robust and stable, they do not have the ability to check the model applicability or estimate the uncertainties of the results. Moreover, the resolution of velocity is relatively low due to the small range of wave number (compared to frequency) from seismic signals or low signal to noise ratio (SNR), especially in cases when signal frequencies or wave numbers overlap (Shen and Li, 2014). In addition, there is no depth information in these spectrums, and the accuracy of the calculated velocity is poor, which seriously hampers the ability to resolve actual geological problems with surface wave.

In order to overcome the deficiencies of the existing methods, we propose a surface wave velocity analysis method in expanded f-k domain that converts the f-k spectrum to velocity analysis spectrum (H-v_R spectrum) with the relationship among frequency, wave number, phase velocity, wavelength, and penetration depth. Then we effectively and easily extracted the phase velocity of surface waves by using the idea of reflected wave velocity analysis. There is quite a straight forward relationship between phase velocity and depth, and we are also able to precisely solve geological problems with interpretation from H-v_R spectrum and H-v_R curve.

METHODOLOGY

f-k transform

Surface wave data $\phi(t, x)$ in the time-space (t-x) domain can be converted to a $\varphi(f, k)$ spectrum in the frequency-wave number (f-k) domain with a 2D Fourier Transform. The mathematical transformation is defined as follows,

$$\begin{cases} \varphi(f,k) = \int_{-\infty}^{+\infty}\int_{-\infty}^{+\infty} \phi(t,x)e^{-i2\pi(ft+kx)}dtdx \\ \phi(t,x) = \int_{-\infty}^{+\infty}\int_{-\infty}^{+\infty} \varphi(f,k)e^{i2\pi(ft+kx)}dfdk \end{cases}, \quad (1)$$

where f is the frequency (Hz), k is the wave number (m^{-1}), t is the traveltime (s), x is propagation space (m), and i is an imaginary unit $\sqrt{-1}$.

Different geological structures, tectonics, elastic properties and other aspects will result in changes in the propagating parameters of surface waves. Some information in the f-k domain is related to geological properties, which is preserved in the seismic response. So based on the abnormal information of relational parameters in f-k spectra, we cannot only study surface wave propagation, but also directly solve practical geological problems.

Rayleigh wave spectrum information in the f-k domain

The amplitude, frequency and wave number of surface waves with different components can be clarified in the f-k domain. The ratio of frequency to wave number reveals the phase velocity information

$$v_R = f/k \quad . \quad (2)$$

We can obtain a v_R-f curve of a certain point by calculating the surface wave phase velocity of different frequency components. It is necessary to further establish the relationship between phase velocity and penetration depth to get a depth-phase velocity (H-v_R) curve for practical applications. Since there is the following relationship among wavelength λ, frequency f and phase velocity v_R,

$$\lambda = v_R/f \quad , \quad (3)$$

and the energy of surface waves mainly focuses in the range of a wavelength,

the penetration depth of surface waves relates to the wavelength. Moreover, there is a relationship between the penetration depth of surface waves and wavelengths,

$$H = \beta\lambda \quad , \tag{4}$$

where H is the penetration depth, β is the depth correction factor, and λ is the wavelength.

According to eqs. (3) and (4), we can further establish the relationship of penetration depth (H) with phase velocity (v_R),

$$H = \beta v_R/f \quad . \tag{5}$$

Heukelom and Foster (1960), and Abbiss (1981) took β equals 0.5 which is the so-called half-wavelength method. It has been verified that the error of the calculated penetration depth with $\beta = 0.5$ is quite serious with a lot of testing (Chen and Sun, 2006; Karray and Lefebvre, 2008; Pan et al., 2013). By assumpting elastic media is homogeneous, and considering the relationship between energy of surface waves and medium characteristics, Chen and Sun (2006) obtained amplitude-penetration depth curves of Poisson's ratio varying from 0.1 to 0.5. Furthermore, they studied the relationship among Poisson's ratio, wavelength and penetration depth of surface waves (Fig. 1). The study showed that the penetration depth of surface waves is from 0.53λ to 0.875λ for all media (Poisson's ratio is from 0.1 to 0.48). For rocks, in general, Poisson's ratio equals 0.25, so the penetration depth approximately is 0.65λ; the Poisson's ratio of Quaternary soil is from 0.4 to 0.45, so the penetration depth is from 0.79λ to 0.84λ.

To build Rayleigh wave velocity spectrum in expanded f-k domain and extract phase velocity

Inspired by the conventional reflected wave velocity analysis method, eqs. (2) and (5) can be further transformed to eq. (6) for seeking the ordinate in the H-v_R domain,

$$\begin{cases} v_R(k_J,f_I) = f_I/k_J & J = -M,-M+1,-M+2,\cdots,0,1,2,\cdots,M \\ H(k_J,f_I) = \beta v_R(k_J,f_I)/f_I & I = -N,-N+1,-N+2,\cdots,0,1,2,\cdots,N \end{cases} , \tag{6}$$

where J and I are the index of the k and f coordinate, respectively, M is the total number of seismic channels after side-expanding, and N is the number of sample per trace after side-expanding. M and N are integer powers of 2. $v_R(k_J,f_I)$ and $H(k_J,f_I)$ represent the coordinate in the H-v_R spectrum.

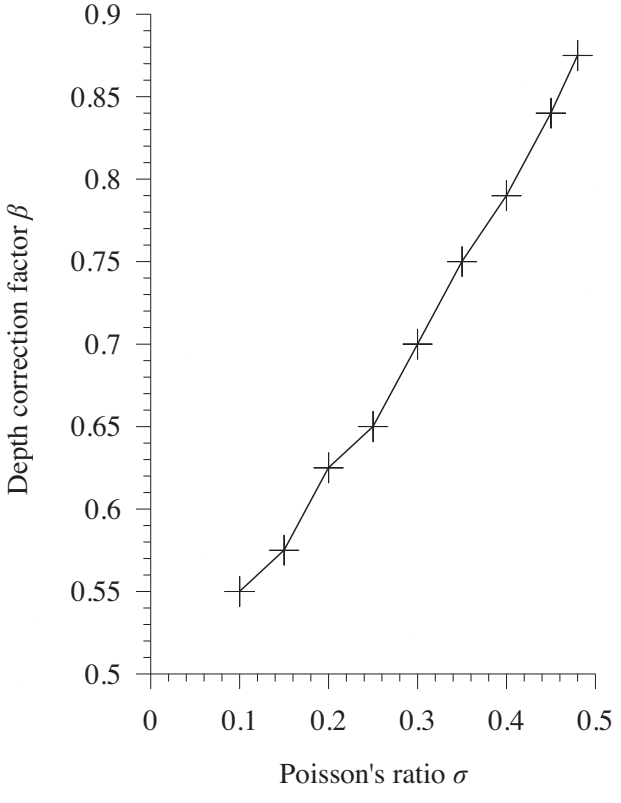

Fig. 1. The relationship between penetration depth correction factor β and Poisson's ratio (based on Chen and Sun, 2006).

It can be seen from Fig. 2a that the phase velocity and penetration depth of each point in the f-k domain can be obtained with eq. (6). It also shows from eq.(2) that multiple phase velocity can be obtained with the slope of every f and k pair. Note that all the points along one slope have the same velocity. Assuming the total number of calculated phase velocity is m, we sorted these phase velocity values in an ascending manner,

$$v_{R1} < v_{R2} < \cdots < v_{Rj} < \cdots < v_{Rm} \quad , \tag{7}$$

where j is the index of phase velocity.

On the other hand, the penetration depth value of each point along a certain f-k slope varies from the others due to different frequencies, although they have the same velocity. We can get the penetration depth on every point with eq. (6). Assuming the number of penetration depth is n, we also sort these penetration depth values in an ascending manner,

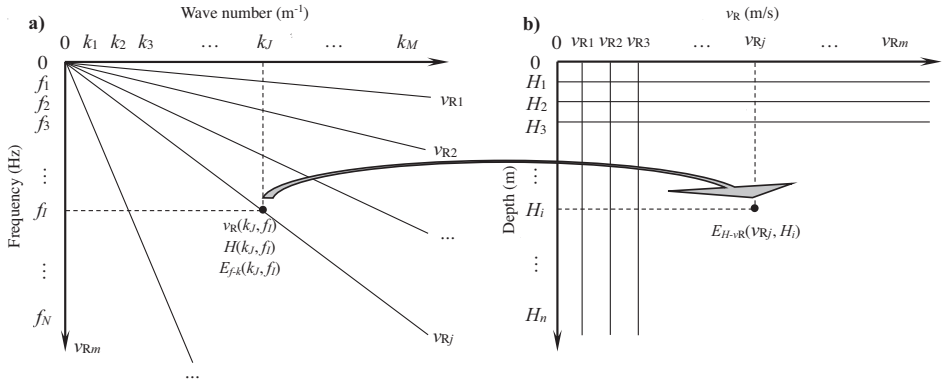

Fig. 2. Schematic diagram of transformation from f-k to H-v_R spectrum.

$$H_1 < H_2 < \cdots < H_i < \cdots < H_n \quad , \tag{8}$$

where i is the index of penetration depth.

The f-k domain has been transformed to the H-v_R domain. Then the energy of each point in the f-k domain also has been mapped to the corresponding coordinates in the H-v_R domain (Fig. 2b). Therefore,

$$E_{f\text{-}k}(k_J,f_I) = E_{H\text{-}v_R}(v_{Rj},H_i) \quad , \tag{9}$$

where $E_{f\text{-}k}(k_J,f_I)$ and $E_{H\text{-}v_R}(v_{Rj},H_i)$ are the energy values in the f-k domain and the H-v_R domain, respectively.

Note, the steps of the calculated initial phase velocity and penetration depth are unequal spacing, so they need to be interpolated when drawing the H-v_R spectrum. In this paper, we used the Kriging interpolation technique.

Fig. 3 is the processing flowchart of multiple-transient surface wave velocity analysis. First, take 2D Fourier transform of the input surface wave data to obtain the f-k spectrum. Second, calculate values of phase velocity $v_R(k_J,f_I)$ at the depth $H(k_J,f_I)$ according to eq. (6), and map the energy value of the (k_J, f_I) in the f-k domain to (v_{Rj},H_i) in the H-v_R domain. Third, obtain the H-v_R dispersion curve of multiple-transient surface wave in the depth-phase velocity domain by picking the maximum energy at each depth. Then, one can get a preliminary assessment of the geological information on site based on the H-v_R dispersion curve.

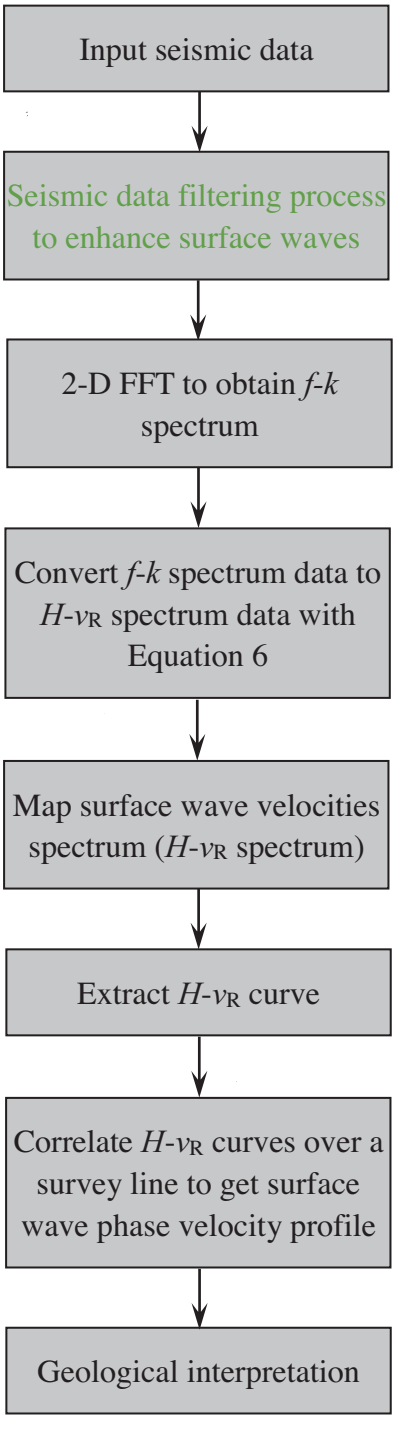

Fig. 3. Processing flowchart for multiple-transient surface wave velocity analysis in the expanded f-k domain.

ACTUAL DATA APPLICATION

Since traditional reflection seismic methods are able to image geologic structures with high resolution for a given survey, it has been widely used to detect active faults (Chow et al., 2001; Ismail et al., 2002; Liu et al., 2012; Shuhab et al., 2013). This technique can not only detect the stratigraphic distribution in a wide range of depths, but it can accurately determine the location, occurrence, and termination of the buried fractures, and so on. Although traditional reflection seismic exploration techniques have many advantages, it also has some drawbacks. The vertical resolution of the methods is limited, to a certain extent, due to the high velocity of the reflected wave. Moreover, it is insensitive to the fractures with small fault throw. In case of active faults that extend to Quaternary strata, the shallow part of the faults is hard to image, due to their small offsets. In addition, the impedance contrast between the Quaternary strata is actually weak, because sediments in shallow depth have not been cemented into solid rocks. Only using the reflected wave information to survey the geological structures above bedrock interface has limitations. The geological information in shallower depth is a key in detecting active faults.

The advantage of surface waves, in comparison to reflected waves, is that it is not affected by the impedance contrast. The response of reflected waves from an interface of a small impedance contrast is weak, so it is difficult to distinguish two layers with the similar impedance. Surface waves do not have this drawback, and its resolution on vertical and lateral is higher. However, the effective depth of surface waves is relatively shallower compared to reflected waves. The resolution will decrease with depth, since the surface wave propagation is confined to a wavelength range. Thus, surface waves can be complementary to reflection seismic studies in detecting active faults. Furthermore, we may use it to solve the geological issues caused by bedrock fracture in Quaternary strata.

In order to take full advantage of seismic data, namely real signals (reflected waves) and "noise" (surface waves) to obtain geological information, we apply the proposed surface wave method to process a set of Rayleigh wave data. The Rayleigh waves were recorded in reflection seismic data for detecting active faults. We intend to better resolve the active faults by jointly using the information from Rayleigh waves and traditional reflection seismic data.

Geological background of work area

The survey is located near the southern Pan Shan Mountains in Jixian region of North China. The topography of this area is flat, and the thickness of

Quaternary sediments is relatively thin. The sediments are mainly from alluvial fan and slope deposits with coarse grains comprise the Quaternary strata. Beneath the Quaternary strata in this area, carbonate rocks are mixed with a small amount of clastics rocks and claystone of the Sinian Jixian group. This geologic configuration ensures that seismic waves will have sufficient energy to reach the bedrock with less attenuation. Moreover, due to a large impedance contrast, the interface between Quaternary strata and bedrock has great reflectivity. Furthermore, fractures in the region are well-developed since the work area is located in the Beijing-Tianjin-Tangshan earthquake belt (Sun and Liu, 1995; Jia, et al., 2009; Jiang, et al., 2013).

Data acquisition

In order to image the contact between bedrock and Quaternary soil and locate faults as well as other structural features near the bedrock, we deployed a reflection seismic line from north to south in this area.

We used the Sercel 428XL telemetry seismic data acquisition system, which was produced in France. The excitation source is longitudinal wave vibrator with maximum output power of 6000 pounds, and a scanning frequency range from 10 to 550 Hz. Seismic data were collected with 21 full coverage containing 84 geophones of a natural frequency of 40 Hz. The channel spacing was 3 m. The minimum offset was 30 m. The shot spacing was 6 m. The sampling rate was 0.5 ms. The recording length was 1 s. The source scanning frequency was from 10 to 120 Hz, and the scanning length was 12 s. The total number of shots was 140.

Seismic data and spectra characteristics analysis

Fig. 4a is a common shot gathers of the 2D seismic line. All kinds of seismic waves are recorded in this dataset. Besides P-P waves, Rayleigh waves are well-developed showing large energy. In addition, direct waves, air blast, and random noises also can be recognized. It is pretty obvious that Rayleigh waves behave quite differently than other seismic waves.

In order to determine the quality of the Rayleigh waves, spectrum analysis is conducted for shot No.65. Fig. 4a is the common shot gather, and Fig. 4b is the filtered Rayleigh wave records from Fig. 4a. Fig. 4c shows the f-k spectrum of Fig. 4b, which does not show a simple relationship, so it is difficult to extract the Rayleigh wave dispersion curve from Fig. 4c with conventional processing methods. However, the distribution of energy group in the H-v_R spectrum (Fig. 4d) is relatively regular, in which the energy distribution is mainly focused in two triangular regions.

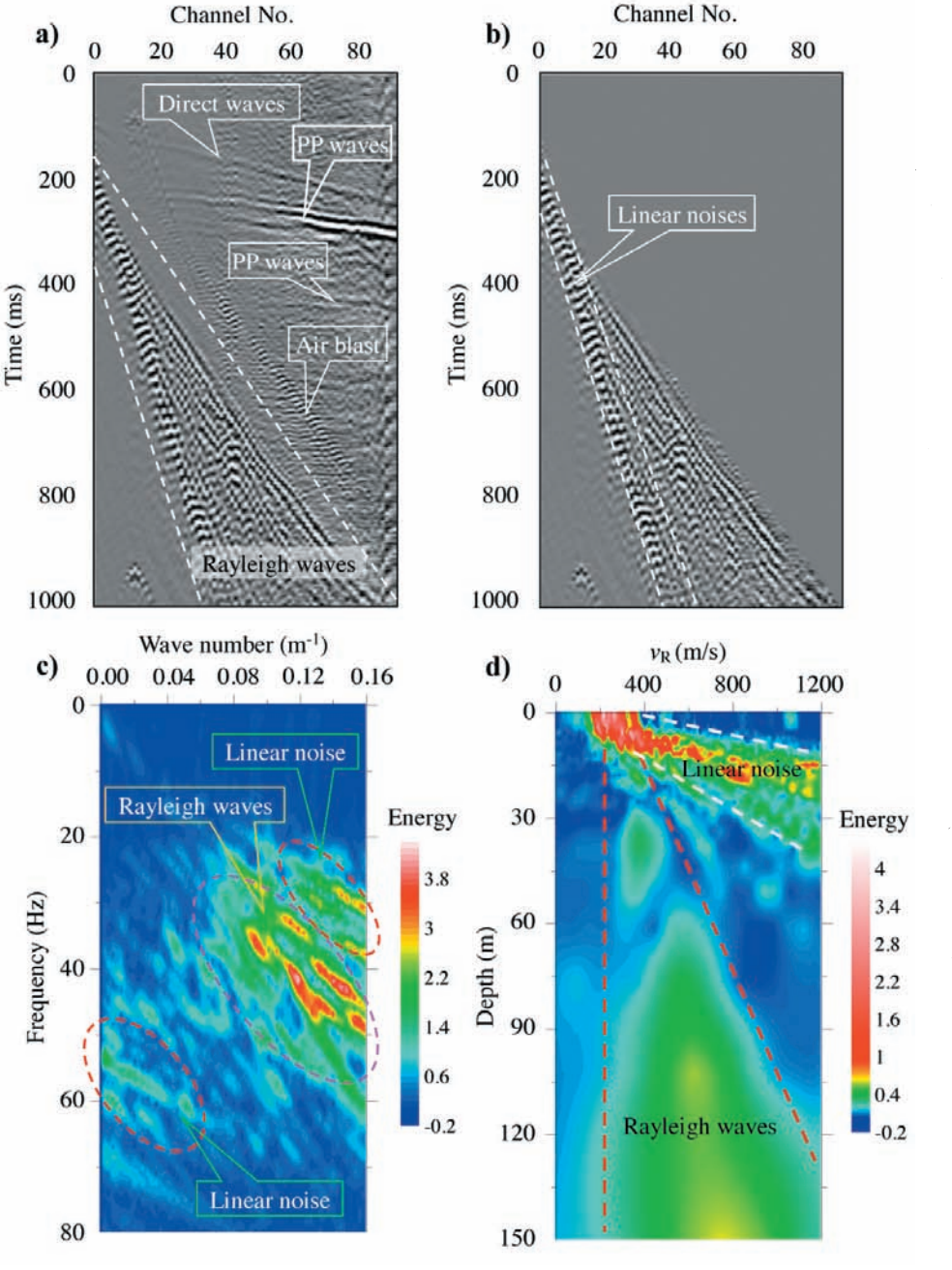

Fig. 4. A typical original seismic records and its spectrums analysis results. a) Raw common shot point gather of Shot No. 65 with developed Rayleigh wave, b) The extracted Rayleigh wave seismic records, c) f-k spectrum of (b), d) H-v_R spectrum of (b).

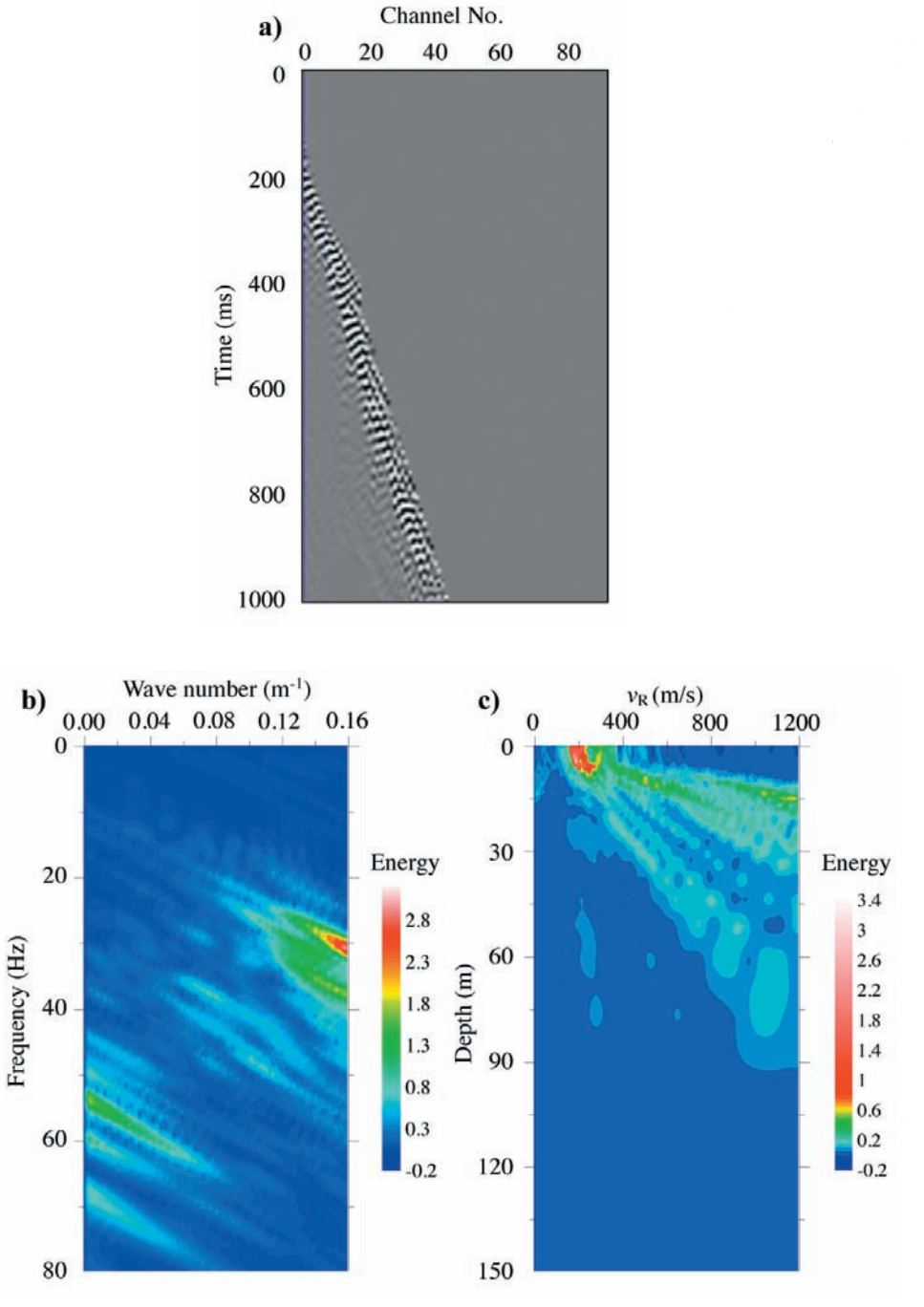

Fig. 5. Linear noise in the Rayleigh waves records and its spectrum analysis results. a) The extracted linear noise from Rayleigh wave records in Fig. 4b, b) The f-k spectrum of (a), c) The H-v_R spectrum of (a).

In Fig. 4b, there is a strong linear noise signature in the Rayleigh waves. Fig. 5a is the filtered linear noise. From the f-k spectrum (Fig. 5b) of this linear noise, one can see that the frequency is from about 25 to 45 Hz and the wave number is from about 0.115 to 0.16 m^{-1}. From the H-v_R spectrum (Fig. 5c), it is obvious that the pattern shows a triangular shape with depths of less than 80 m, and the velocity ranges from 200 to 1200 m/s. Comparing Figs. 5c and 4d, those upper triangular patterns are very consistent, so we can conclude that the anomaly in lower triangular region of Fig. 4d is caused by the Rayleigh waves. Such linear noises belong to ground roll waves that are formed by the difference in velocities between two formations. In seismic wave propagation process, a part of seismic energy has been blocked to spread to the underground by the velocity difference interface between loose weathered layer and dense phreatic aquifer. The blocked seismic energy continued to propagate in loose weathered layer and formed ground roll waves with the features of lower velocity, strong energy and lower frequencies.

Rayleigh wave data processing

After trying several correction factor β, we considered that the correction factor β of 0.79 is more reasonable to build a H-v_R spectrum, because the near surface Quaternary soil overlies bedrock in the area. Figs. 6a and 6b show the H-v_R spectrum of shot No. 1 and No. 40, respectively, and their corresponding H-v_R curves. From these figures, the Rayleigh wave patterns are more regular with strong energy groups and high signal to noise ratio. Also, it is obvious to see several layers with different phase velocity. Generally, phase velocity increases with depth, but a shallow low-velocity layer is showed in the H-v_R spectrum of shot No. 1 from 82 to 135 m. We obtained the Rayleigh wave phase velocity profile by connecting each H-v_R curves for all shots of the line, as shown in Fig. 7a.

Results analysis

The reflected wave data were also processed for comparison. The corresponding relationship of the first and last detection points between multiple-transient surface waves and CDP of reflected waves are in the Appendix. It can be seen from the reflection wave imaging section (Fig. 7b) that the top of bedrock is clear. The top of bedrock dips from north to south, with traveltime of about 160 ms to the north and 240 ms to the south. From the reflected wave velocity spectrum of CMP No. 70 (Fig. 8), it can be seen that the bedrock velocity is about 1750 m/s near 210 ms. Then we infer the depths of the top of the bedrock to be from about 136 m (north) to 204 m (south). Furthermore, a series of minor faults can be seen from the reflection seismic cross-section in this region, and a fracture zone is also identified from CDP No.

570 to CDP No. 620. However, the seismic information above the bedrock is unobserved.

Although the Rayleigh wave H-v_R profile (Fig. 7a) cannot completely define the bedrock top, some structures above the bedrock are very obvious with clear velocity interfaces and local anomalies. Moreover, significant vertical and lateral velocity variations indicate that the bedrock fractures have affected the depositional structures above bedrock. According to the Rayleigh wave phase velocity profile (Fig. 7a), we may identify two possible interfaces with velocities of 360 m/s and 720 m/s. Based on the local geology, we speculated that the 360 m/s surface is the water table top, and the 720 m/s surface is the top of the deceleration zone. Comparing with the reflection seismic cross-section in Fig. 7b, both have the same dipping trend from north to south. Moreover, all the faults that were imaged in the reflection seismic cross-section are consistent with the velocity anomalies in Fig. 7a. In addition, the low phase velocity zone at the south end in Fig. 7a is also consistent with the fracture zone indicated in the reflection seismic cross-section. Overall, most structures and trends in the reflection seismic cross-section can be correlated with indicators from the H-v_R profile.

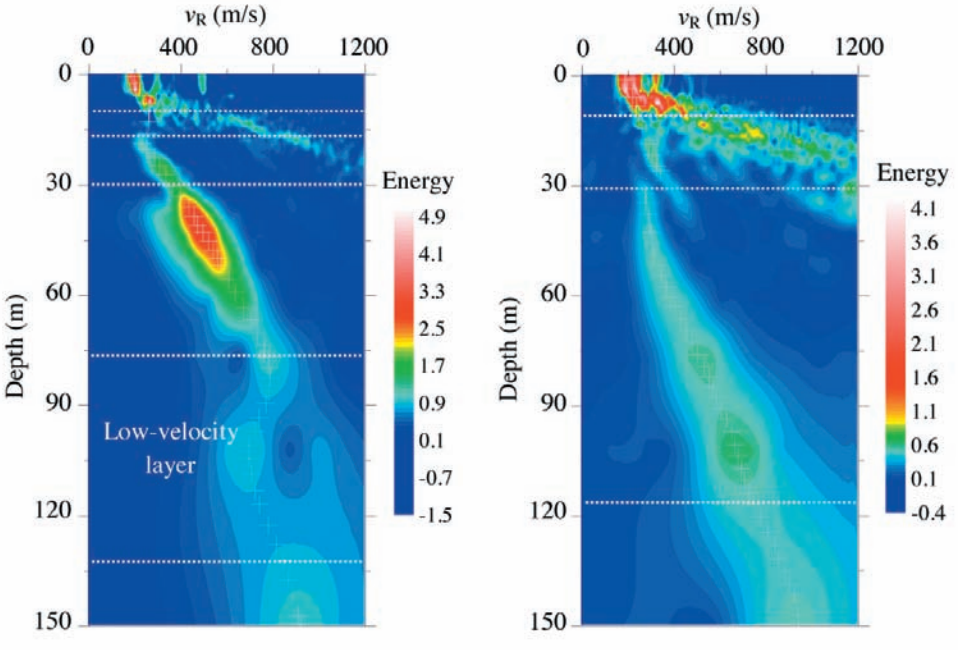

Fig. 6. Two typical shots of Rayleigh wave velocity spectrums and their H-v_R curves. a) The Rayleigh wave H-v_R spectrum of the Shot No. 1 and the extracted H-v_R curve, b) The Rayleigh wave H-v_R spectrum of the Shot No. 40 and the extracted H-v_R curve.

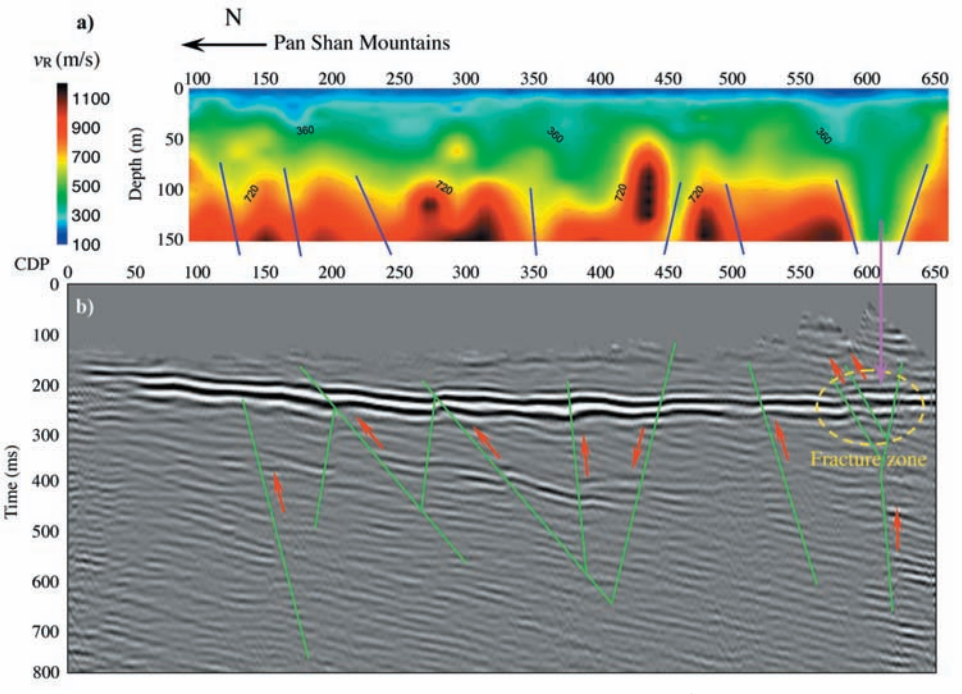

Fig. 7. Seismic data interpretation. a) Rayleigh wave phase velocity profile with interpretation, b) Reflection seismic image section with interpretation.

DISCUSSION AND CONCLUSIONS

We have developed a new method of multiple-transient surface wave velocity analysis. Testing with a real seismic data, we have made several conclusions based on our understanding, which are as follows:

1. Based on the relationship among phase velocity, frequency, and wave number, as well as the relationship between penetration depth and wavelength, the f-k spectrum of multiple-transient surface waves may be converted into a H-v_R spectrum. The effectiveness of the spectrum is similar to the traditional reflected wave velocity spectrum. Surface wave H-v_R spectrum offers clear information about phase velocity with depth relation. Furthermore, velocity analysis is relatively easier for multiple-transient surface wave processing. We first mention surface wave H-v_R spectrum for shallow depth velocity imaging. Currently, other types of traditional surface wave data processing techniques do not have the concept of a velocity spectrum.

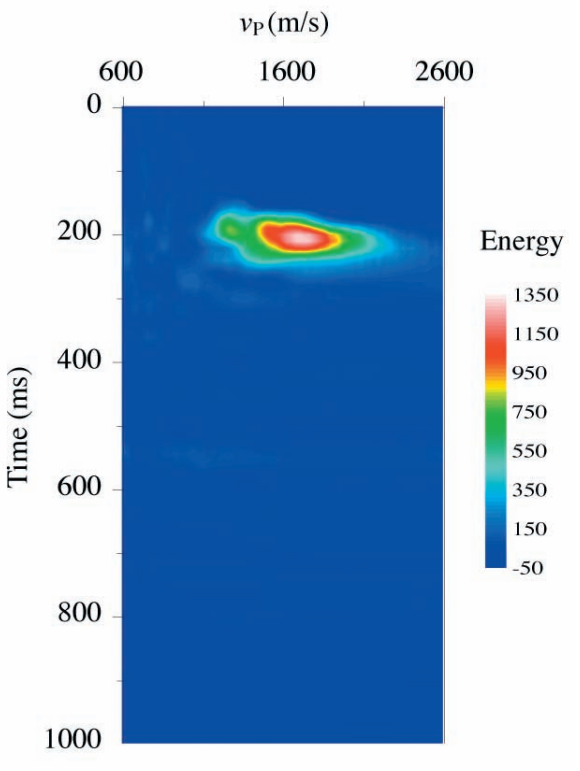

Fig. 8. Reflected wave velocity spectrum of the CMP No. 70.

2. In the f-k spectrum, surface waves with different frequencies and the same velocity are separated. So it is not convenient to fully utilize the information carried by the spectrum to obtain information from traditional methods. However, in the H-v_R spectrum, surface waves with different frequencies and the same velocity are stacked together. It can not only effectively enhance the signal coherence, but also make full use of the information carried by seismic records. Therefore, this method can greatly improve the de-noising ability of surface wave velocity analysis.

3. By converting the wave number-frequency domain to a phase velocity-penetration depth domain, we stack the corresponding energy and map them into the H-v_R spectrum and extract the strongest energy that ensures the surface wave velocity accuracy.

4. Selecting the correct or approximate factor β, which determines the depth in our method, is significantly critical to the accuracy of the surface wave analysis, since eventually phase velocity is dependent on depth. Furthermore, β is empirically determined by Poisson's ratio, which is

related to the local geology. Therefore, before conducting any study with this method, how well one can know the geology and the range of Poisson's ratio in a study area will determine the reliability of the processing results.

5. Compared with the traditional surface wave data processing in the f-k domain, the information of velocity versus depth relationship in the H-v_R domain is more straightforward, also the accuracy is relatively higher. Application to real data also shows that the de-noising capability of this method is also very strong. In addition, the H-v_R spectrum reflects surface wave energy change that indicates attenuation level when the seismic waves travel through geological bodies. Therefore, this spectrum can obtain surface wave phase velocity with high accuracy.

6. Seismic exploration has different goals for different target depths. Detecting active faults with high accuracy is an important topic in shallow exploration. The reflected waves are useful for detecting deep structures, while the surface waves can be used to image the velocities for shallower depths, such as geological structures in Quaternary strata, instead of being regarded as noise. So, if surface waves are well developed in seismic data, they are useful in offering more information. With surface wave and reflected wave processing, a more complete geological picture can be obtained.

ACKNOWLEDGEMENTS

This research is supported by the PetroChina Innovation Foundation (#2014D-5006-0303), and Key Laboratory Research Project of the Shaanxi Provincial Department of Education (#13JS093). We also thank Dr. G. Randy Keller, Tengfei Lin and Xiao Xu for giving us some suggestions. And many thanks to Dr. Jefferson Chang for his editing and reviewing effort of this paper.

REFERENCES

Abbiss, C.P., 1981. Shear wave measurements of the elasticity of the ground. Geotechnique, 31: 91-104. doi: 10.1680/geot.1981.31.1.91.

Boiero, D., Wiarda, E. and Vermeer, P., 2013. Surface- and guided-wave inversion for near-surface modeling in land and shallow marine seismic data. The Leading Edge, 32: 638-646. doi:10.1190/tle32060638.1.

Chen, X. and Sun, J., 2006. An improved equivalent homogenous half-space method and reverse fitting analysis of Rayleigh wave dispersion curve. Chin. J. Geophys., 49: 569-576.

Chow, J., Angelier, J., Hua, J.J., Lee, J.C. and Sun, R., 2001. Paleoseismic event and active faulting: from ground penetrating radar and high-resolution seismic reflection profiles across the Chihshang Fault, eastern Taiwan. Tectonophysics, 333: 241-259. doi:10.1016/S0040-1951(00)00277-8.

Gabriels, P., Snieder, R. and Nolet, G., 1987. In situ measurements of shear-wave velocity in sediments with higher-mode Rayleigh wave. Geophys. Prosp., 35: 187-196. doi: 10.1111/j.1365-2478.1987.tb00812.x.

Gucunski, N. and Woods, R., 1992. Numerical simulation of the SASW test. Soil Dynam. Earthq. Engin., 11: 213-227. doi:10.1016/0267-7261(92) 90036-D.

Haskell, N.A., 1953. The dispersion of surface wave on multilayered media. Bull. Seismol. Soc. Am., 43: 17-34.

Heukelom, W. and Foster, C., 1960. Dynamic testing of pavements. J. Soil Mechan. Foundat. Div., 86: 1-28 (SM1).

Ismail, K., Makoto, O., Hiromi, M. and Yasuo, A., 2002. Active faults in the Gulf of Izmit on the North Anatolian Fault, NW Turkey: a high-resolution shallow seismic study. Marine Geol., 190: 421-443. doi:10.1016/S0025-3227(02)00357-2.

Jia, H., He, Z. and Ye, T., 2010. Application of SASW and MASW to buried fault detection. Progr. Geophys. (in Chinese), 25: 709-713. dio:10.3969/j.issn.1004- 2903.2010.02.046.

Jia, S., Zhang, C., Zhao, J., Fang, S., Liu, Z. and Zhao, J., 2009. Crustal structure of the rift-depression basin and Yanshan uplift in the northeast of North China. Chin. J. Geophys. (in Chinese), 52: 99-110.

Jiang, D., Jiang, W. and Hu, W., 2013. Study of crustal structure and geodynamic characteristics around the Bohai Sea area. Progr. Geophys. (in Chinese), 28: 1729-1738. doi:10.6038/pg20130413.

Karray, M. and Lefebvre, G., 2008. Significance and evaluation of Poisson's ratio in Rayleigh wave testing. Can. Geotech. J., 45: 624-635. doi:10.1139/T08-016.

Liu, B., Zhao, C., Feng, S., Yang, X., He, Y., Li, W., Zou, Y. and Kou, K., 2012. Application of the three-component shallow seismic reflection method to probing buried active faults. Chin. J. Geophys. (in Chinese), 58: 2676-2686. doi:10.6038/j.issn.0001- 5733.2012.08.020.

Mari, L., 1984. Estimation of static corrections for share-wave profiling using the dispersion properties of love waves. Geophysics, 49: 1169-1179. doi:10.1190/1.3479491.

Matthews, M.C., Hope, V.S. and Clayton, C.R.I., 1996. The use of surface wave in the determination of ground stiffness profiles. Proc. Inst. Civ. Eng. Geotech. Eng., 119: 84-95.

McMechan, G.A. and Yedlin, M.J., 1981. Analysis of dispersive waves by wave field transformation. Geophysics, 46: 869-874. doi:10.1190/1.1441225.

Pan, Y., Xia, J., Gao, L., Shen, C. and Zeng, C., 2013. Calculation of Rayleigh-wave phase velocities due to models with a high-velocity surface layer. J. Appl. Geophys., 96: 1-6. http://dx.doi.org/10.1016/j.jappgeo.2013.06.005.

Park, C.B., Mille, R.D. and Xia, J., 1996. Multi-channel analysis of surface wave using Vibroseis (MASWV). Expanded Abstr., 66th Ann. Internat. SEG Mtg., Denver: 68-71.

Park, C.B., Mille, R.D. and Xia, J., 1998. Imaging dispersion curves of surface wave on multi-channel record. Expanded Abstr., 68th Ann. Internat. SEG Mtg., New Orleans: 1377-1380.

Park, C.B., Mille, R.D. and Xia, J., 1999. Multichannel analysis of surface wave. Geophysics, 64: 800-808. doi:10.1190/1.1444590.

Rayleigh, L., 1887. On waves propagated along the plane surface of an elastic solid. Proc. London Mathemat. Soc., 17: 4-11.

Ritzwoller, H.M. and Levshin, A.L., 2002. Estimating shallow shear velocities with marine multicomponent seismic data. Geophysics, 67: 1991-2004. doi: 10.1190/1.1527099.

Shen, H. and Li, Q., 2014. One new Rayleigh wave velocity analysis method. Proc. 6th Internat. Conf. Environm. Engineer. Geophys., Xi'an, China: 121-125.

Shuhab, D.K., Robert, R.S., Maisam, O. and Li, C., 2013. A geophysical investigation of the active Hockley Fault System near Houston, Texas. Geophysics, 78: B177-B185. doi:10.1190/GEO2012-0258.1.

Stokoe II, K.H. and Nazarian, S., 1983. Effectiveness of ground improvement from spectral analysis of surface wave. Proc. 8th Europ. Conf. Soil Mechanics Foundat. Engineer., Helsinki, Finland: 91-95.

Strobbia, C. and Foti, S., 2006. Multi-offset phase analysis of surface wave data (MOPA). J. Appl. Geophys., 59: 300-313. doi:10.1016/j.jappgeo.2005.10. 009.

Strobbia, C., Emam, A.E., Al-Genai, J. and Roth, J., 2010. Rayleigh wave inversion for the near-surface characterization of shallow targets in a heavy oil field in Kuwait. First Break, 28: 103-109.

Strobbia, C., Laake, A., Vermeer, P. and Glushchenko, A., 2011. Surface wave: use them then lose them. Surface-wave analysis, inversion and attenuation in land reflection seismic surveying. Near Surf. Geophys., 9: 503-514. doi: 10.3997/1873-0604.2011022.

Sun, R. and Liu, F., 1995. Crust structure and strong earthquake in Beijing, Tianjing, Tangshan area. Part I: P-wave velocity structure. Chin. J. Geophys. (in Chinese), 38: 599-607.

Xia, J., Miller, R. and Park, C.B., 1999. Estimation of near-surface shear-wave velocity by inversion of Rayleigh wave. Geophysics, 64: 691-700. doi:10.1190/ 1.1444578.

Xia, J., Chen, C., Tian, G., Miller, R.D. and Ivanov, J., 2005. Resolution of high-frequency Rayleigh-wave data. J. Environ. Eng. Geophys., 10: 99-110. doi:10.2113/ JEEG10.2.99.

Xia, J., 2014. Estimation of near-surface shear-wave velocities and quality factors using multichannel analysis of surface-wave methods. J. Appl. Geophys., 103: 140-151. http://dx.doi.org/10.1016/j.jappgeo.2014.01.016.

APPENDIX A

CORRESPONDING RELATIONSHIP BETWEEN DETECTION POINT OF MULTIPLE-TRANSIENT SURFACE WAVES AND COMMON DEPTH POINT (CDP) OF REFLECTED WAVES

Due to the different detection mechanisms between multiple-transient surface waves and reflected waves, the detection points of the two techniques are not the same when the source-receiver configuration is the same. The CDP of reflected waves is the center point of the source and receiver, but the detection point of multiple-transient surface waves is the center point of the first and last trace for each shot. In order to compare the velocity analysis results of the multiple-transient surface waves and the cross section of reflection seismic imaging, it is necessary to know the corresponding relationship of detection points between these two techniques.

Corresponding relationship of the first detection point between them

As shown in Fig. A-1, assuming m channels per shot, a minimum offset L, the channel interval Δx and the relative coordinates of the first shot is 0, so the CDP interval is

$$\Delta x_{CDP} = \Delta x/2 \quad . \tag{A-1}$$

The coordinate of the first CDP is

$$x_1 = L/2 \quad . \tag{A-2}$$

The coordinate of the first detection point of multiple-transient surface waves is

$$x_2 = [(m - 1)\cdot\Delta x/2] + L \quad . \tag{A-3}$$

Then we can derive the CDP number of reflected waves corresponding to the first detection point of multiple-transient surface waves, which is

$$m_1 = (x_2 - x_1)/\Delta x_{CDP} = (L/\Delta x) + m - 1 \quad . \tag{A-4}$$

In this paper, the minimum offset L is 30 m, channel interval Δx is 3 m, and total channels per shot m are 84. Therefore, we obtain that m_1 equals 93. This means that the first detection point of multiple-transient surface waves of the first shot corresponds to the CDP No. 93 of reflection seismic image.

Corresponding relationship of the last detection point between them

Similarly, we can get the corresponding relationship of the last detection point between multiple-transient surface waves and reflected waves as well. As shown in Fig. A-1(b), the total channel per shot is m, the minimum offset distance is L, the channel interval is Δx, and the relative coordinates of the last shot is also 0, then the coordinate of the last CDP of Reflected wave is

$$x_m = [(m - 1) + L]/2 \quad . \tag{A-5}$$

The coordinate of the last detection point of multiple-transient surface waves is

$$x_3 = [(m - 1)\cdot\Delta x/2] + L \quad . \tag{A-6}$$

Therefore, we can calculate the number of the last detection point of multiple-transient surface waves exceeding the last CDP of reflected waves from

$$m_2 = (x_3 - x_m)/\Delta x_{CDP} = L/\Delta x \quad . \tag{A-7}$$

In this paper, the minimum offset L is 30 m, and channel interval Δx is 3 m, so we can obtain m_2 equals 10. This means that the last shot detection point of multiple-transient surface waves exceeds the last CDP of the reflection seismic image by 10 channels.

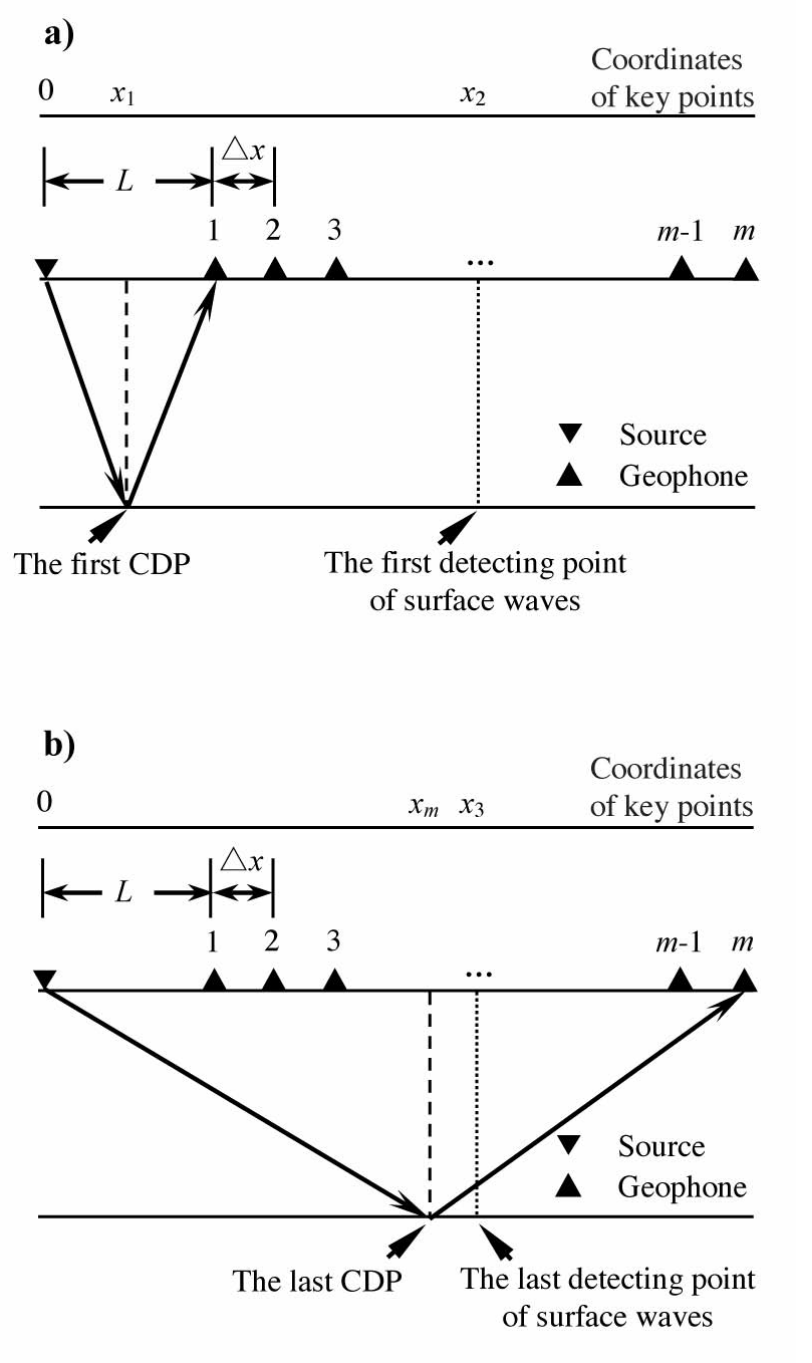

Fig. A-1. Scheme of detecting points between multiple-transient surface waves and reflected waves. a) The first detecting points of multiple-transient surface waves and reflected waves, b) The last detecting points of multiple-transient surface waves and reflected waves.